

Meson and baryon elliptic flow at high p_T from parton coalescence

Dénes Molnár

Department of Physics, Ohio State University, Columbus, OH 43210

Abstract. The large and saturating differential elliptic flow $v_2(p_\perp)$ observed in $Au + Au$ reactions at RHIC so far could only be explained assuming an order of magnitude denser initial parton system than estimated from perturbative QCD. Hadronization via parton coalescence can resolve this “opacity puzzle” because it enhances hadron elliptic flow at large p_\perp relative to that of partons at the same transverse momentum. An experimentally testable consequence of the coalescence scenario is that $v_2(p_\perp)$ saturates at about 50% higher values for baryons than for mesons. In addition, if strange quarks have weaker flow than light quarks, hadron v_2 at high p_\perp decreases with relative strangeness content.

PACS numbers: 12.38.Mh; 24.85.+p; 25.75.Gz; 25.75.-q

1. Introduction and summary

Differential elliptic flow, $v_2(p_\perp) \equiv \langle \cos(2\phi) \rangle_{p_\perp}$, the second Fourier moment of the azimuthal momentum distribution for a given p_\perp , is one of the important experimental probes of collective dynamics in $A + A$ reactions[1]. Measurements of elliptic flow at high transverse momentum provide important constraints about the opacity of the partonic medium in heavy-ion collisions[2, 3, 4].

Recent data from RHIC for $Au + Au$ reactions at $\sqrt{s_{NN}} = 130$ and 200 GeV show a remarkable saturation property of elliptic flow for $\sim 2 \text{ GeV} < p_\perp < \sim 6 \text{ GeV}$ with v_2 reaching up to 0.2 [6, 5, 8, 7], a value that corresponds to a factor of two azimuthal angle asymmetry of particle production relative to the reaction plane. As illustrated in Fig. 1, the saturation pattern differs qualitatively from calculations based on a variety of different models: ideal (nondissipative) hydrodynamics[9, 11, 10, 12], hadronic cascades with string dynamics[13], inelastic parton energy loss[2], and classical Yang-Mills evolution[14].

On the other hand, covariant parton transport theory[15, 16, 18, 17, 3, 19] is able to reproduce the observed flow saturation pattern. The main ingredient of this theory is a finite local mean free path $\lambda(s, x) \equiv 1/\sigma(s)n(x)$, providing a natural interpolation between free streaming ($\lambda = \infty$) and ideal hydrodynamics ($\lambda = 0$). Several studies show that initial parton densities and elastic $2 \rightarrow 2$ parton cross sections estimated from perturbative QCD, $dN_g/d\eta(b = 0) \sim 1000$ [20] and $\sigma_{gg \rightarrow gg} \approx 3 \text{ mb}$, generate too small collective effects at RHIC[16, 17, 3, 19]. Nevertheless, quantitative agreement with the $v_2(p_\perp)$ data is possible, provided initial parton densities and/or cross sections are enhanced by an order of magnitude to $\sigma dN_g/d\eta(b = 0) \sim 45\,000 \text{ mb}$ [3]. An

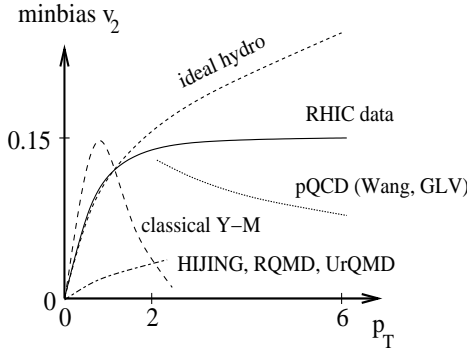


Figure 1. Illustrative comparison between $v_2(p_\perp)$ data from RHIC and model calculations[2, 14, 9, 11, 10, 12, 13].

enhancement of parton opacities seems necessary to explain the pion interferometry data from RHIC as well[19].

To compare to the experiments, parton transport models have to incorporate the hadronization process. The studies mentioned above considered two simple schemes: 1) $1\text{parton} \rightarrow 1\pi$ hadronization, motivated by parton-hadron duality, and 2) independent fragmentation. An alternative is parton coalescence[21], which became the focus of recent theoretical interest[22, 23, 25, 4, 24] as a possible explanation for the anomalous meson/baryon ratio and features of the elliptic flow data at RHIC. These studies indicate that hadron production at RHIC may be dominated by coalescence out to surprisingly large transverse momenta $p_\perp \sim 5$ GeV.

In this talk I show that hadronization via parton coalescence can resolve the opacity puzzle because it leads to an amplification of elliptic flow[4] at high p_\perp (see Fig. 2a). With this enhancement, parton transport calculations[3] can account for the charged particle elliptic flow data from RHIC with moderate initial parton densities and cross sections $dN_g/d\eta \sim 1500 - 3000$, $\sigma_{gg \rightarrow gg} = 3$ mb.

Parton coalescence predicts a rather simple relationship, Eq. (2), between parton flow coefficients and those of hadrons. If all partons have similar elliptic flow, elliptic flow is stronger for baryons than for mesons, $v_2^B \approx 1.5v_2^M$, at high $p_\perp > 2 - 3$ GeV, as shown in Fig. 2a. If on the other hand strange quarks show weaker flow than light quarks, elliptic flow at high p_\perp is ordered by relative strangeness content, such that $v_2^p > v_2^\Lambda \approx v_2^\Sigma > v_2^\pi > v_2^K > v_2^\phi$, $v_2^{\Lambda, \Sigma} > v_2^\Xi > v_2^K$, and $v_2^\Xi > v_2^\Omega \approx 3v_2^\phi/2$ (see Fig. 2b). These predictions are reinforced by preliminary calculations using the MPC parton transport model[26] (see Fig. 3a) and can be readily tested in current and future heavy-ion collision experiments.

With the help of (2), one can also determine the elliptic flow of the various parton species from v_2 measurements for several hadrons, providing valuable insight on the evolution of the dense parton medium in heavy-ion collisions.

2. Parton coalescence

A convenient framework to start with is the local variant of the coalescence model[22, 4], in which the coalescing partons have equal momenta. This is justified if hadron wave functions are narrow in momentum space and if constituent partons

have similar masses. See Ref. [24] for a study of the more general case.

Assuming that all partons have the same momentum distribution, the hadron spectra at midrapidity are then given by

$$\frac{dN_B}{d^2p_\perp}(\vec{p}_\perp) = C_B(p_\perp) \left[\frac{dN_q}{d^2p_\perp}(\vec{p}_\perp/3) \right]^3, \quad \frac{dN_M}{d^2p_\perp}(\vec{p}_\perp) = C_M(p_\perp) \left[\frac{dN_q}{d^2p_\perp}(\vec{p}_\perp/2) \right]^2, \quad (1)$$

where C_M and C_B are the probabilities for $q\bar{q} \rightarrow \text{meson}$ and $qqq \rightarrow \text{baryon}$ coalescence. The coefficients C can in general depend on momentum, for example, if there is a strong radial flow.

Equation (1) is valid for rare processes only. At high constituent phase space densities, most quarks recombine into hadrons and the number of hadrons is *linearly* proportional to that of quarks, $dN_h(p_\perp) \propto dN_q(p_\perp/n)$ ($n = 2, 3$ for mesons, baryons).

At lower constituent densities, parton coalescence is relatively rare and Eq. (1) is applicable. Clearly, most partons hadronize via independent fragmentation in this case. Still, hadron production can be dominated by coalescence in a broad region of *hadron* transverse momenta. The reason is that in independent fragmentation hadrons with a given p_\perp come from rare high-momentum partons with momentum p_\perp/z ($z < 1$), i.e., $dN_h^{frag}(p_\perp) \sim dN_q(p_\perp/z)$, whereas via coalescence they can come from more abundant low-momentum partons with momenta p_\perp/n , i.e., $dN_h^{coal}(p_\perp) = C_h[dN_q(p_\perp/n)]^n$.

At very high transverse momenta, the fragmentation process wins because due to the quadratic/cubic dependence in Eq. (1) the coalescence yield drops steeper as a function of p_\perp than the fragmentation yield. E.g., a power law parton spectrum $dN_q/p_\perp dp_\perp \sim Ap_\perp^{-\alpha}$ implies $dN_h^{coal}/dN_h^{frag} \sim C_h A^{n-1} p_\perp^{-(n-1)\alpha} \rightarrow 0$ at high p_\perp . The boundary between the coalescence and fragmentation regions may be at rather large transverse momenta $p_\perp \sim 5$ GeV[25].

3. Elliptic flow amplification and ordering

In the coalescence region, meson and baryon elliptic flow are given by that of partons via[4]

$$v_{2,M}(p_\perp) \approx 2v_{2,q}\left(\frac{p_\perp}{2}\right), \quad v_{2,B}(p_\perp) \approx 3v_{2,q}\left(\frac{p_\perp}{3}\right), \quad (2)$$

as follows from Eq. (1) and $v_2 \ll 1$. For example, if partons have only elliptic anisotropy, i.e., $dN_q/p_\perp dp_\perp d\Phi = (1/2\pi)dN_q/p_\perp dp_\perp[1 + 2v_{2,q} \cos(2\Phi)]$, then

$$v_{2,B}(p_\perp) = \frac{3v_{2,q}(p_\perp/3) + 3v_{2,q}^3(p_\perp/3)}{1 + 6v_{2,q}^2(p_\perp/3)}, \quad v_{2,M}(p_\perp) = \frac{2v_{2,q}(p_\perp/2)}{1 + 2v_{2,q}^2(p_\perp/2)}. \quad (3)$$

Note, Eq. (2) is also valid for all flow coefficients $v_k \equiv \langle \cos k\phi \rangle$, not only v_2 .

Fig. 2a illustrates the effect of parton coalescence on baryon and meson elliptic flow, as given by Eq. (2), compared to parton elliptic flow. The latter is shown schematically by the solid line. At small transverse momenta, parton $v_2(p_\perp) \propto p_\perp^2$, as follows from general analyticity considerations. This region, before v_2 becomes approximately linear in p_\perp could be relatively small (depending on the effective mass of partons). At higher transverse momenta $p_\perp > 1 - 2$ GeV, parton elliptic flow saturates as predicted by the MPC parton transport model[3].

In the low- p_\perp region where $v_2(p_\perp)$ increases faster than linearly, $v_{2,B} < v_{2,M} < v_{2,q}$. Though here Eq. (2) may not be applicable, it is nevertheless interesting that the data do exhibit such a behavior. This ordering follows naturally from hydrodynamics,

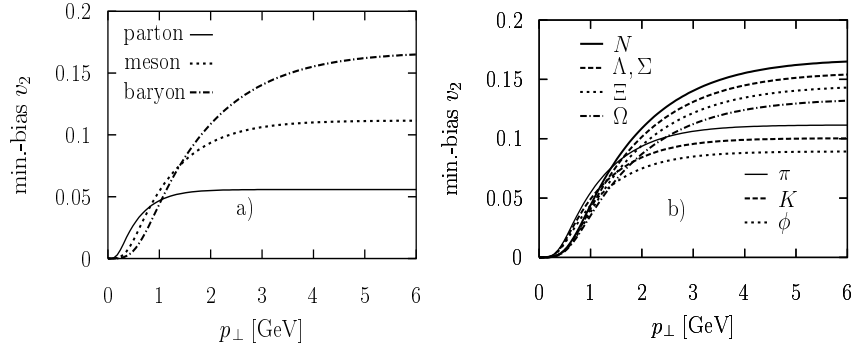


Figure 2. Qualitative behavior of baryon and meson elliptic flow as a function of p_\perp from parton coalescence, a) if all partons have the same v_2 , b) if $v_2^s < v_2^q$.

where flow decreases with increasing particle mass[9, 11, 10]. Similar mass dependence could also arise in a coalescence model because heavier hadrons can be formed by quarks with larger relative momentum (ignored in the local coalescence approach).

On the other hand, at high p_\perp , where parton $v_2(p_\perp)$ increases slower than linearly, baryon flow becomes larger than meson flow, $v_{2,B} > v_{2,M} > v_{2,q}$, by as much as 50%. Parton collective flow saturation above $p_\perp > 1 - 2$ GeV results in saturating meson/baryon flow at $p_\perp > 2 - 4$ GeV that is *amplified two/three-fold* compared to that of partons. Saturation sets in at 50% higher p_\perp for baryons than for mesons. Note that any eventual decrease of parton elliptic flow at very high p_\perp (e.g., because of parton energy loss) would happen at two to three times larger p_\perp for hadrons.

The high- p_\perp results above strongly differ from those obtained in Ref. [23]. The reason is that, unlike Eq. (2), in Ref. [23] the coalescence of quarks was considered to be independent of their relative momenta and therefore hadron elliptic flow at high p_\perp was similar to that of a high- p_\perp quark.

If not all partons show the same elliptic flow, further differentiation occurs because in that case

$$\begin{aligned} v_{2,B=abc}(p_\perp) &\approx v_{2,a}(p_\perp/3) + v_{2,b}(p_\perp/3) + v_{2,c}(p_\perp/3) \\ v_{2,M=\bar{a}b}(p_\perp) &\approx v_{2,\bar{a}}(p_\perp/2) + v_{2,b}(p_\perp/2) . \end{aligned} \quad (4)$$

For example, strange quarks may have a smaller $v_2(p_\perp)$ than light quarks, at high p_\perp because heavy quarks are expected to lose less energy in nuclear medium[27], while at low p_\perp due to the mass dependence of hydrodynamic flow. As illustrated in Fig. 2b, if $v_2^s < v_2^q$, elliptic flow decreases with increasing relative strangeness content within the baryon and meson bands, i.e., $v_2^p > v_2^\Lambda \approx v_2^\Sigma > v_2^{\Xi} > v_2^\Omega$ and $v_2^\pi > v_2^K > v_2^\phi$.

The above conclusions are also supported by detailed numerical calculations using the MPC parton transport model[26]. Fig. 3a shows the elliptic flow results for $Au + Au$ with $b = 8$ fm at $\sqrt{s} = 200A$ GeV at RHIC, computed from the azimuthal distribution of hadrons obtained via Eq. (1). The initial parton spectra, shown in Fig. 3b, were computed from leading-order perturbative QCD (GRV98LO, BKK95, $K = 2.5$, $Q^2 = p_\perp^2$) with a cutoff $p_0 = 2$ GeV, below which the spectra were continued smoothly down to $p_\perp = 0$ to yield a p_\perp -integrated parton density $dN/d\eta = 2000$ at $\eta = 0$. The parton cross sections were $\sigma_{gg \rightarrow gg} = 3$ mb = $(9/4)\sigma_{qg \rightarrow qg} = (9/4)^2\sigma_{qq \rightarrow qq}$. The preliminary calculation shows rather small difference between the elliptic flow of strange and light quarks. Surprisingly, v_2^s is slightly larger than v_2^q , however, this may

be because flavor changing channels $gg \leftrightarrow qq$ and $q_i q_i \rightarrow q_j q_j$ were not included.

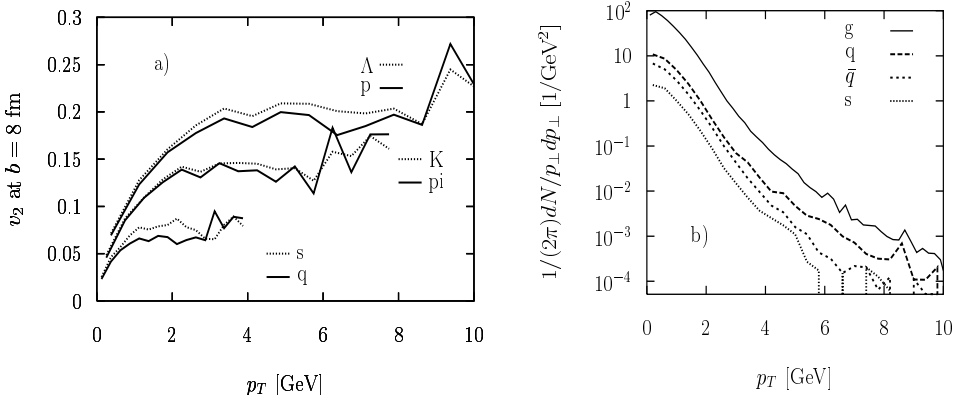


Figure 3. a) Preliminary elliptic flow ordering results from the MPC parton transport model[26]. b) Initial parton spectra for the MPC simulations.

4. Solution to the opacity puzzle

While hadronization via $1\text{parton} \rightarrow 1\pi$ or independent fragmentation approximately preserves elliptic flow at high $2 < p_\perp < 6$ GeV [3], parton coalescence enhances v_2 two times for mesons and three times for baryons. Hence, the same hadron elliptic flow can be reached from 2 – 3 times smaller parton v_2 , i.e., with smaller parton densities and/or cross sections.

To determine the reduction of the parton opacity quantitatively, one can utilize the results of Ref. [3] that computed gluon elliptic flow as a function of the transport opacity, $\chi \equiv \int dz \sigma_{tr} \rho(z) \approx \sigma dN/d\eta / (940 \text{ mb})$, from elastic parton transport theory for a minijet scenario of Au+Au at $\sqrt{s} = 130A$ GeV at RHIC. Those results can be conveniently parameterized as $v_2(p_\perp, \chi) = v_2^{max}(\chi) \tanh[p_\perp/p_0(\chi)]$, where v_2^{max} is the saturation value of elliptic flow, while p_0 is the p_\perp scale above which saturation sets in. For the estimates here one may assume that all gluons convert, e.g., via $gg \rightarrow qq$, to quarks of similar p_\perp and hence $v_2^q(p_\perp) = v_2^g(p_\perp)$.

Because the increase of elliptic flow with opacity is weaker than linear[3, 4], $v_2^{max} \sim \chi^{0.61}$, the charged particle v_2 data from RHIC can be reproduced in the coalescence scenario with 3 – 6 times smaller parton opacities $\sigma dN/d\eta(b = 0) \sim 7000 – 15000$ mb than those found in Ref. [3]. The lower(upper) value applies if high- p_\perp hadrons are mostly baryons(mesons). Preliminary PHENIX data [28] show $\pi_0/h^\pm \approx 0.5$ between $2 < p_\perp < 9$ GeV, therefore one may expect $\text{mesons/baryons} \approx 1$, in which case $\sigma dN/d\eta(b = 0) \approx 10\,000$ mb.

In Ref. [3] only collective flow was considered and the parton opacity at RHIC was extracted using elliptic flow data from the reaction plane analysis. Taking into account non-flow effects that contributed up to 15-20% [29] to the first elliptic flow measurements, parton opacities should be further reduced by 25% to $\sigma dN/d\eta(b = 0) \sim 5000 – 10000$ mb. For a typical elastic $gg \rightarrow gg$ cross section of 3 mb, this corresponds to an initial parton density $dN/d\eta(b = 0) \sim 1500 – 3000$, only 1.5 – 3 times above the EKRT perturbative estimate[20].

The remaining much smaller discrepancy is within theoretical uncertainties. For example, perturbative cross section and parton density estimates may be too low. If most hadrons form via coalescence, the observed hadron multiplicity $dN_h/d\eta \approx 1000$ would imply higher initial parton densities $dN/d\eta \sim 2000 - 3000$. Constituent quark cross sections, $\sigma_{qq} \approx 4 - 5$ mb, also point above the ≈ 3 mb perturbative estimate. One effect that estimate ignores is the enhancement of parton cross sections $\sigma \propto \alpha_s^2/\mu^2$ due to the decrease of the self-consistent Debye screening mass $\mu \sim gT_{eff}(\tau)$ during the expansion. Finally, the contribution of inelastic processes, such as $gg \leftrightarrow ggg$, to the opacity has also been neglected so far. A preliminary study shows[17] that this contribution can be similar to that of elastic processes.

Acknowledgments

Valuable comments by U. Heinz and M. Gyulassy and computer resources by the PDSF/LBNL are gratefully acknowledged. This work was supported by DOE grants DE-FG02-01ER41190 and DE-FG02-92ER40713.

References

- [1] For a recent review see, e.g.: J. Ollitrault, Nucl. Phys. A **638**, 195 (1998); A. M. Poskanzer, nucl-ex/0110013; or Ref. [22].
- [2] X. Wang, Phys. Rev. C **63**, 054902 (2001); M. Gyulassy, I. Vitev and X. N. Wang, Phys. Rev. Lett. **86**, 2537 (2001); M. Gyulassy *et al.*, Phys. Lett. B **526**, 301 (2002).
- [3] D. Molnar and M. Gyulassy, Nucl. Phys. A **697**, 495 (2002); Erratum-*ibid* A **703**, 893 (2002).
- [4] D. Molnar and S. A. Voloshin, nucl-th/0302014.
- [5] C. Adler *et al.* [STAR Collaboration], Phys. Rev. Lett. 90, 032301 (2003). *ibid* **89**, 132301 (2002); *ibid* **87**, 182301 (2001).
- [6] K. Adcox [PHENIX Collaboration], Phys. Rev. Lett. **89**, 212301 (2002).
- [7] S. Esumi [PHENIX Collaboration], nucl-ex/0210012.
- [8] K. Filimonov [STAR Collaboration], Nucl. Phys. A **715**, 737 (2003).
- [9] P. F. Kolb, J. Sollfrank and U. W. Heinz, Phys. Lett. B **459**, 667 (1999); Phys. Rev. C **62**, 054909 (2000).
- [10] D. Teaney, J. Lauret and E. V. Shuryak, Phys. Rev. Lett. **86**, 4783 (2001).
- [11] P. F. Kolb *et al.*, Nucl. Phys. A **696**, 197 (2001); Phys. Lett. B **500**, 232 (2001); P. Huovinen *et al.*, Phys. Lett. B **503**, 58 (2001).
- [12] U. W. Heinz and P. F. Kolb, hep-ph/0204061.
- [13] H. Sorge, Nucl. Phys. **A661**, 577 (1999); M. Bleicher and H. Stocker, Phys. Lett. B **526**, 309 (2002).
- [14] A. Krasnitz, Y. Nara and R. Venugopalan, Phys. Lett. B **554**, 21 (2003).
- [15] B. Zhang, Comput. Phys. Commun. **109**, 193 (1998).
- [16] B. Zhang, M. Gyulassy and C. M. Ko, Phys. Lett. **B455**, 45 (1999).
- [17] D. Molnár, Nucl. Phys. **A661**, 236 (1999).
- [18] D. Molnár and M. Gyulassy, Phys. Rev. C **62**, 054907 (2000).
- [19] D. Molnár and M. Gyulassy, nucl-th/0211017.
- [20] K. J. Eskola *et al.*, Nucl. Phys. **B570**, 379 (2000).
- [21] T. S. Biro, P. Levai and J. Zimányi, Phys. Lett. B **347**, 6 (1995); P. Csizmadia and P. Levai, J. Phys. G **28**, 1997 (2002).
- [22] S. A. Voloshin, nucl-ex/0210014.
- [23] Z. w. Lin and C. M. Ko, Phys. Rev. Lett. **89**, 202302 (2002).
- [24] Z. w. Lin and D. Molnár, nucl-th/0304045.
- [25] R. J. Fries *et al.*, nucl-th/0301087; V. Greco, C. M. Ko and P. Levai, nucl-th/0301093.
- [26] D. Molnár, MPC 1.6.0. This parton cascade code can be downloaded from WWW at <http://www-cunuke.phys.columbia.edu/people/molnard>.
- [27] Y. L. Dokshitzer and D. E. Kharzeev, Phys. Lett. B **519**, 199 (2001); M. Djordjevic and M. Gyulassy, Phys. Lett. B **560**, 37 (2003).
- [28] S. Mioduszewski [PHENIX Collaboration], nucl-ex/0210021.
- [29] C. Adler *et al.* [STAR Collaboration], Phys. Rev. C **66**, 034904 (2002).